Molecular Neurobiology

ISSN0893-7648/98/20(1): 17–28/$13.00

Local Accumulations of B-50/GAP-43 Evoke Excessive Bleb Formation in PC12 Cells

L. H. J. Aarts,[1] P. Verkade,[3] L. H. Schrama*,[2], A. B. Oestreicher†,[2], W. H. Gispen,[2] and P. Schotman[1]

[1]Department of Physiological Chemistry, Rudolf Magnus Institute for Neurosciences, Utrecht University, Universiteitsweg 100, 3584 CG Utrecht, The Netherlands; [2]Department of Medical Pharmacology, Rudolf Magnus Institute for Neurosciences, Utrecht University, Universiteitsweg 100, 3584 CG Utrecht, The Netherlands; and [3]Cell Biology and Biophysics Programme, European Molecular Biology Laboratory, Meyerhoferstrasse 1, D-69012 Heidelberg, Germany and Max Planck Institute for Molecular Cell Biology and Genetics, Dresden, Germany

Abstract

B-50 (GAP-43) is an axonal, plasma membrane-associated protein involved in growth cone morphology and function. We have conducted immunocytochemical, electron microscopic, and time-lapse experiments to visualize morphological consequences of local accumulations of B-50 at the plasma membrane of B-50-transfected PC-B2 cells, a clonal PC12 cell line with very low expression of endogenous B-50. The distribution of the transfected B-50 within these cells was inhomogeneous. At sites where the B-50 concentration was locally increased up to twofold, numerous filopodia were present in growth cone-like, substrate-attached regions. When local B-50 concentrations were even higher (up to 6.2-fold), blebs were formed, often containing vesicular structures, heavily decorated with B-50 immunoreactivity. Double labeling with f-actin binding phalloidin revealed that local B-50 accumulations were accompanied by increased actin filament concentrations. Colocalization of B-50 with actin filaments was prominent in filopodia, but was virtually absent in blebs, suggesting a disconnection of the bleb plasma membrane from the actin cytoskeleton. We conclude that B-50 evokes distinct effects on cell-surface activity in PC12 cells depending on its local concentration.

Index Entries: B-50; GAP-43; blebs; filopodia; f-actin; morphology; PC12.

Abbreviations: EM, electron microscopy; EGFP, enhanced green fluorescent protein; f-actin, filamentous actin, FITC, fluorescein isothiocyanate; GAP, growth-associated protein; NGF, nerve growth factor; PBS, phosphate-buffered saline; PC12, pheochromocytoma 12; PKC, protein kinase C.

* Author to whom all correspondence and reprint requests should be addressed.

† During the preparation of this manuscript, we lost our colleague A. Beate Oestreicher after a courageous struggle against a fatal disease. With her we lost a very engaging and warm coworker and friend who is deeply missed.

Introduction

Initiation of neurite outgrowth is characterized by the upregulation of expression of a limited number of growth-associated proteins (GAPs), including the axonal, plasma membrane-associated protein B-50 *(1,2)*. Direct evidence supporting an important role for B-50 in growth cone function and neurite outgrowth has been obtained by manipulating B-50 expression levels in a variety of nonneuronal and neuronal cells. Heterologous expression of B-50 in nonneuronal cells evoked spontaneous formation of numerous cell-surface extensions and influenced cell spreading *(3–7)*. Overexpression of B-50 in neuronal cells increased stimulus-induced neurite outgrowth *(8,9)* as well as neurite stability *(10)*. Conversely, downregulation of B-50 expression with antisense oligonucleotides or interference with its function by introduction of anti-B-50 antibodies reduced or prevented neurite outgrowth *(11–14)*.

Rat pheochromocytoma (PC12) cells form a well-characterized model to study neuritogenesis *(15)*. Treatment with nerve growth factor (NGF) induces neurite outgrowth, which is accompanied by enhanced B-50 expression and a translocation from intracellular organelles, including multivesicular bodies and lysosomal structures, to the plasma membrane *(16)*. Overexpression of B-50 in PC12 cells caused spontaneous formation of filopodia and blebs *(17)*, increased the complexity of growth cones *(18)*, and enhanced stimulus-induced neurite outgrowth *(9)*. PC12 subclones deficient in B-50 expression still exhibited NGF-induced neurite outgrowth, suggesting that the presence of B-50 is not a prerequisite for neuritogenesis *(19)*. However, downregulation of B-50 expression in PC12 cells or primary dorsal root ganglion neurons with antisense B-50 oligonucleotides reduced growth cone complexity and attenuated neurite outgrowth and steering, implying an important regulatory role for B-50 in growth cone morphology and function *(11,12,18)*.

The B-50 protein is coupled to membranes rapidly after its synthesis via palmitoylation of two N-terminal cysteines *(20)*. The integrity of these cysteines is essential for sorting of B-50 to the plasma membrane *(21–24)* and for its morphogenetic activity *(3,4,25)*. However, the molecular determinants underlying the morphological effects of B-50 in neuronal cells remain largely unknown. B-50 colocalizes to a large extent with cortical actin filaments *(3,12,17,25)*, and in vitro cosedimentation studies suggest that B-50 may actually associate with actin filaments *(26–28)*. We have conducted a series of transfection experiments in NGF-differentiated PC-B2 cells to examine:

1. The relation between local B-50 concentrations and local cell-surface morphology.
2. The effects of B-50 on the local actin filament concentration and organization.
3. The ultrastructural localization of B-50 within these extensions.
4. The dynamics of B-50-induced cell-surface extensions.

From these experiments, we conclude that accumulations of B-50 at the plasma membrane evokes a local reorganization of the peripheral actin cytoskeleton, resulting in the formation of motile filopodia and growth cone-like structures or in turbulent membrane blebbing, depending on the local B-50 concentration.

Materials and Methods

Cell Culture, Transfection, and Immunocytochemistry

PC-B2 cells were grown essentially according to Greene et al. *(15)*, as described before *(17)*. Cells were transfected with wild-type (wt) rat B-50 cDNA in pcDNA1 (Invitrogen, San Diego, CA) using lipofectin (Life Technologies, BRL, Gaithersburg, MD). Subsequently, cells were differentiated in chemically defined medium (N1) supplemented with β-NGF (10 ng/mL; Boehringer Mannheim, Germany) and insulin (5 μg/mL; Sigma Chemical, St. Louis, MO). After 2 d, cells were fixed in 4% paraformaldehyde and 0.05% glutaraldehyde and immunolabeled for B-50, using specific monoclonal antibodies (MAbs) (NM4; 1 : 4000 *[29]*). F-actin was visualized by including FITC-coupled phalloidin (Sigma) during incu-

bation with the secondary antibody. Cells were observed with an upright Leica TCS-NT confocal laser scanning microscope (Heidelberg, Germany). To demonstrate colocalization of B-50 and f-actin, the respective red and green signals were merged resulting in a yellow color in case of colocalization.

Pre-embedment Immunogold Labeling of B-50-Transfected PC-B2 Cells

PC-B2 cells were grown on collagen-coated thermanox cover slips (Life Technologies), transfected and differentiated for 48 h as described above. Cells were fixed for 20 min with 4% paraformaldehyde and 0.05% glutaraldehyde in 0.1 *M* phosphate buffer at pH 7.4, washed, and incubated for 1 h in PBS plus 0.1% Na azide, 0.1% saponin, and 5% normal goat serum. Subsequently, cells were incubated overnight with NM4 (1:4000) in the same buffer, washed, and incubated for 1 h with 1-nm gold particles attached to antimouse immunoglobulins (1:100; Aurion, Wageningen, the Netherlands). Cells were then fixed with 2% glutaraldehyde in PBS for 30 min, washed, and postfixed in 0.5% osmium tetroxide for 30 min. After thorough rinsing in tridistilled water, the 1-nm gold particles were silver-enhanced for 30 min, according to the procedure of Danscher *(30)*. Subsequently, cover slips were washed and contrasted with uranyl acetate (4%), dehydrated in ethanol, and embedded in Epon. Finally, sections were examined in a Philips CM10 electron microscope. Local intracellular membrane-bound B-50 levels were quantified by comparing the number of gold particles per μm of membrane length at smooth membrane surfaces with the number of gold particles per μm of membrane length at surface extensions.

Time Lapse

PC-B2 cells were grown on 24-mm, collagen-coated glass cover slips, transfected with pB-50/enhanced green fluorescent protein (EGFP) *(3)*, a construct bearing the open reading frame of B-50 cloned directly upstream of EGFP in pEGFP-N1 (Clontech, Palo Alto, CA), and differentiated with NGF for 48 h. Time-lapse recordings were performed at 37°C and 7% CO_2 in a microchamber mounted on an inverted Leica TCS NT confocal laser scanning microscope (Heidelberg, Germany). After identification of green fluorescing cells, indicative of expression of the B-50/EGFP-fusion construct, time-lapse recordings were started with time intervals of 10 s.

Results

Morphogenetic Activity of B-50 in Transfected PC-B2 Cells

To study the morphogenetic activity of B-50 in neuronal cells, we have examined changes in morphology on overexpression of B-50 in NGF-differentiated PC-B2 cells, a PC12 cell line expressing very low levels of endogenous B-50 *(17)*. Transient transfection of PC-B2 cells with wild-type (wt)B-50 cDNA evoked a clear morphological change toward a phenotype with numerous filopodia and/or blebs in cells expressing enhanced levels of B-50 (Fig. 1) compared to untransfected cells. Blebs were hardly ever observed in transfected PC-B2 cells expressing wt B-50 at levels comparable to that in parental PC12 cells (not shown) or in cells transfected with Ser_3Gly_4-B-50, a mutant that fails to attach to the plasma membrane (not shown) *(3)*. Transiently transfected PC-B2 cells expressing B-50 levels that are clearly higher than wt PC12 cells displayed two different phenotypes. The first phenotype displayed filopodia (Fig. 1A, B, lower transfected cell) and/or veil-like extensions (Fig. 1B, upper transfected cell). The extensions were mostly concentrated at discrete, growth cone-like areas at the cell surface (Fig. 1A, B), The corresponding phalloidin staining revealed that B-50 and actin filaments were coconcentrated and colocalized at these morphologically active sites (Fig. 1A, B, right panel, yellow color). Untransfected cells displayed an overall smooth cell surface with lower levels of corti-

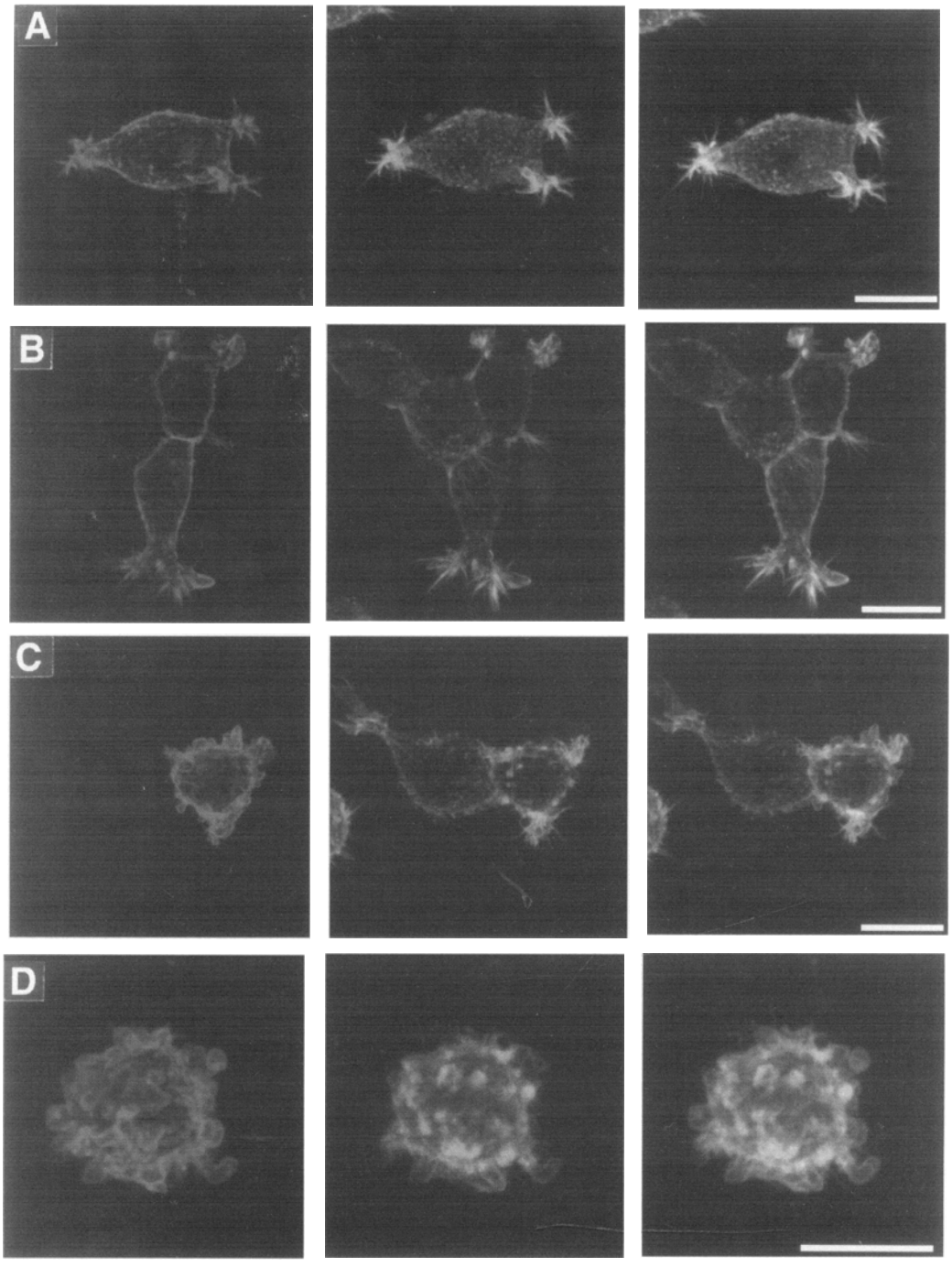

Fig. 1. B-50-induced formation of cell-surface protrusions in PC-B2 cells. PC-B2 cells were transfected with B-50 cDNA and grown for 48 h in the presence of NGF. Cells were fixed and double-labeled with B-50 antibodies (left panels) and with f-actin binding phalloidin-FITC (middle panels). Right panels show the overlay of B-50 and f-actin. **A** and **B:** Transfected cells displaying filopodia or veils extending from growth cone-like structures. **C** and **D:** Transfected cells with high levels of B-50 expression displaying prominent blebbing. Scale bars, 10 μm.

cal actin and virtual absence of local f-actin accumulations (Fig. 1B, left two cells). In the second phenotype, the surface of B-50-transfected PC-B2 cells displayed both filopodia and blebs (Fig. 1C) or was entirely covered with blebs (Fig. 1D). Blebs varied considerably in size and shape, ranging from globular to flask-like with the occasional appearance of secondary or even tertiary blebs on top of a primary bleb (Fig. 1D). Again, the cortical actin filament concentrations were increased in transfected, blebbing cells when compared to surrounding nontransfected cells (Fig. 1C). However, the actin filament concentration appeared to differ between individual blebs: whereas most small blebs contained high amounts of actin filaments throughout the bleb interior, large blebs were virtually devoid of f-actin, although some phalloidin staining was detected near the plasma membrane (Fig. 1D, middle panel). This did not reflect differences in localization or concentration of B-50, since both small and large blebs displayed enhanced levels of B-50, located primarily at the plasma membrane (Fig. 1C, and D; left panel). Virtually no colocalization could be observed between B-50 and actin filaments (Fig. 1D; virtual lack of yellow color).

Ultrastructural Localization of B-50 in Transfected PC-B2 Cells

To examine the ultrastructure of B-50-induced cell-surface extensions and the relative abundance and localization of B-50 within these extensions, we performed pre-embedment immunogold electron microscopy (EM) on B-50-transfected PC-B2 cells. Transfected cells could be identified from nontransfected cells by the presence of many gold particles where untransfected cells hardly contained any gold particles. Figure 2A shows a representative example of a B-50-transfected cell with filopodial extensions. Within these cells, most gold particles were localized in the immediate vicinity of the plasma membrane with very few B-50 gold particles in the cytosol. The gold particle concentration appeared to be elevated at morphologically active regions, i.e., at sites with numerous small rod-like structures, reminiscent of filopodia (Fig. 2A). On quantitation of various filopodial cells, the amount of gold particles was elevated 1.1- to 2-fold at the plasma membrane of filopodial extensions compared to smooth (morphologically inactive) regions of the plasma membrane. At higher magnification, gold particles within filopodia appeared to be associated predominantly with the lipid bilayer (inset 2B).

Other cells clearly contained a much higher concentration of B-50 gold particles than transfected cells with filopodia (compare Fig. 2A and B). These cells with very high concentrations of B-50 often exhibited an irregular shape with large bulbous structures, presumably representing blebs (Fig. 2B, C). Many of the B-50 immunoreactive gold particles were located at or near bleb plasma membranes, whereas morphologically inactive sites (smooth surfaces) were again low in gold particle concentration (Fig. 2C). On quantitation, the amount of gold particles was locally 1.7- to 6.2-fold higher at blebbing membranes. Whereas the interior of some blebs had the same morphological appearance as the cellular cytosol and seemed to be in contact with the cellular cytosol (Fig. 2B), others had a more electron light structure and thus appeared isolated (Fig. 2C). In the latter case, a small strand of B-50 decorated membranous material bordered the bleb interior from the cytosol (Fig. 2C and inset). Strikingly, the bleb interior often contained numerous large, electron-lucent membranous structures covered with gold particles (Fig. 2C). At higher magnification, these structures were bordered by a lipid bilayer, confirming their membranous nature (Fig. 2C; inset, arrow).

Motility of B-50-Induced Protrusions

In order to study the motility of the B-50-induced cell-surface extensions, we performed time-lapse experiments on living cells transfected with a B-50/EGFP-fusion construct. The use of this construct allowed high-resolution

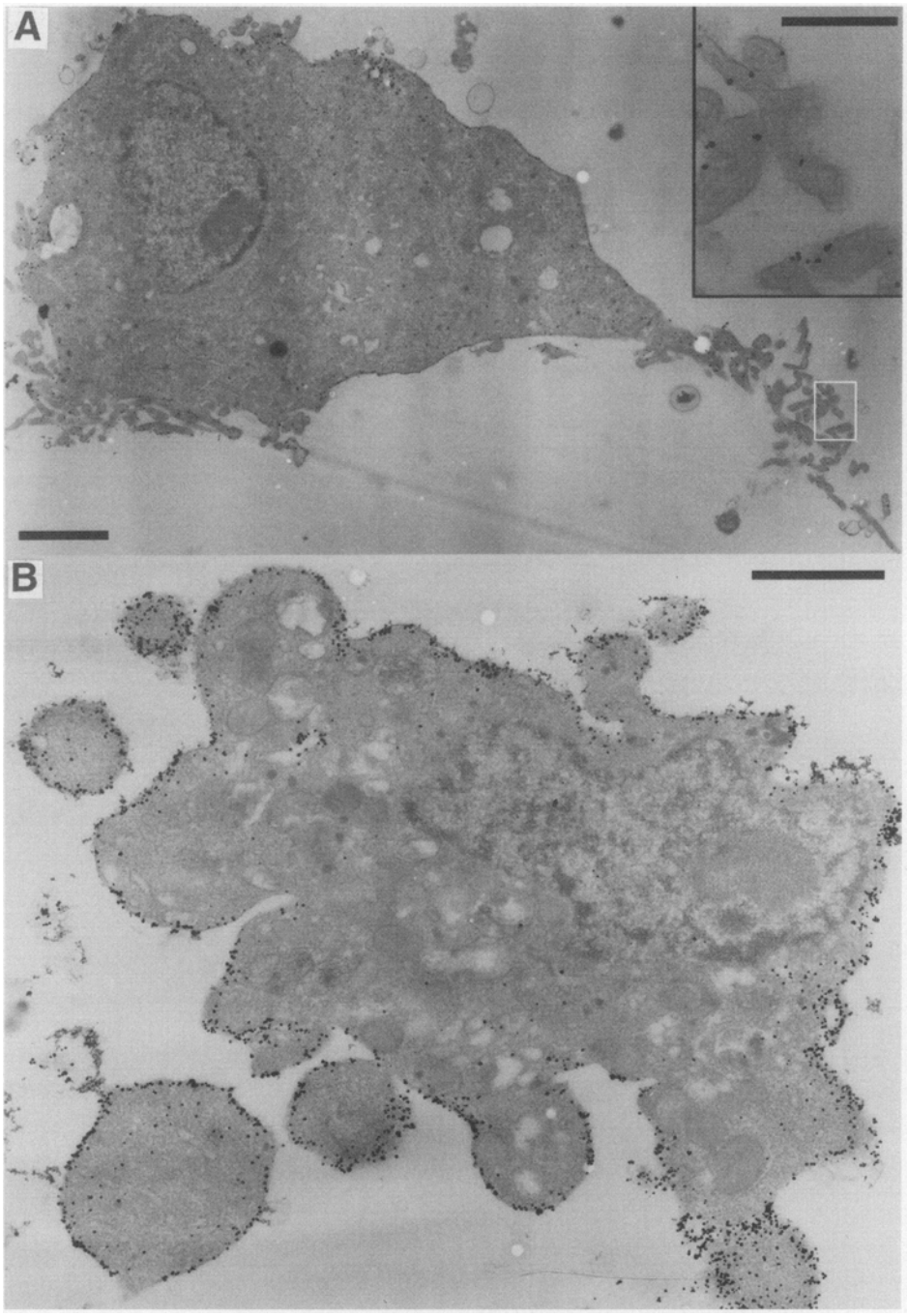

Fig. 2. Ultrastructural immunolocalization of B-50 in transfected PC-B2 cells. PC-B2 cells were treated as described in the legend to Fig. 1 and processed for pre-embedment immuno-EM. **A:** B-50-transfected cell displaying filopodia. Inset shows an enlargement of the boxed area. **B** and **C:** Transfected cells with high local levels of B-50 displaying prominent blebbing. Inset in C shows an enlargement of the boxed area. Scale bars **A, B,** and **C:** 2 μm; scale bar insets: 0.5 μm. *(Figure continues)*

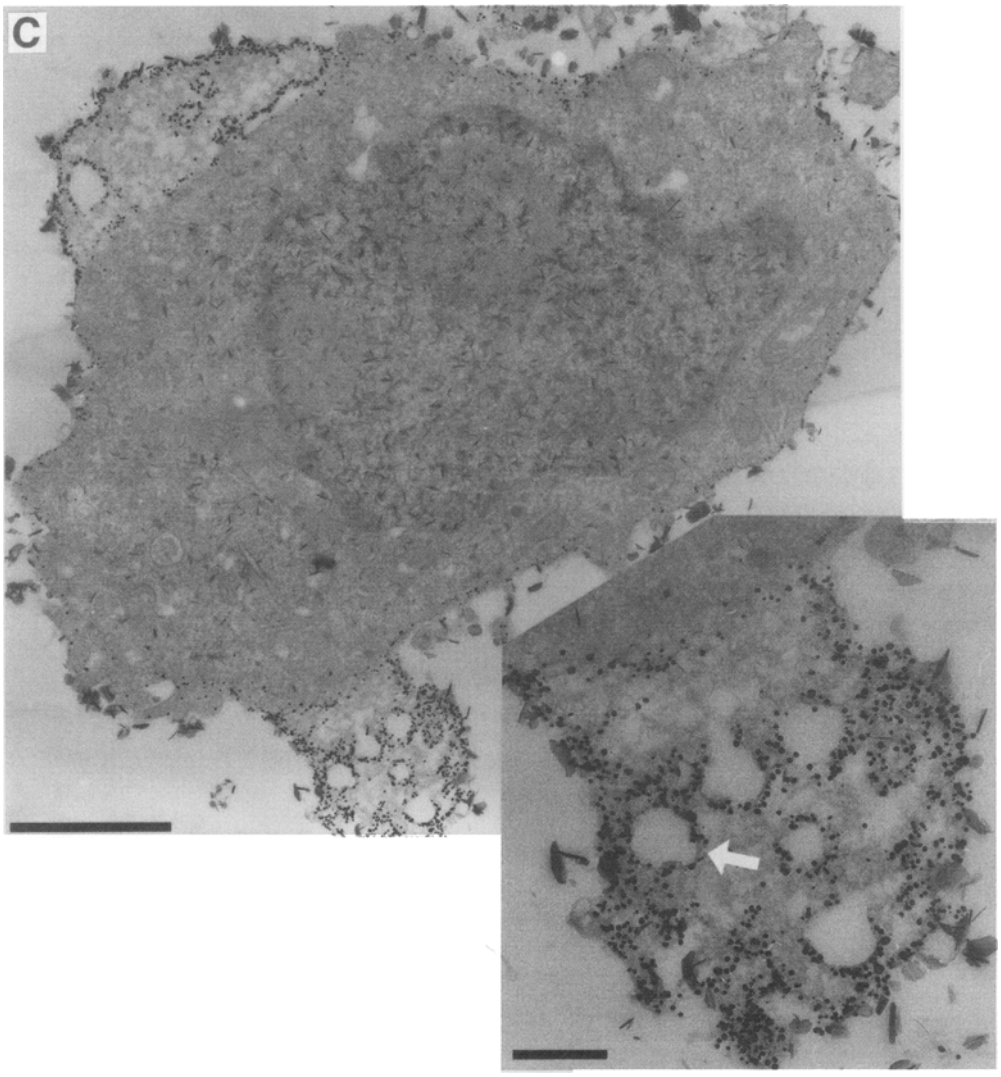

Fig. 2. Continued

examination of cell-surface dynamics at sites of B-50 accumulation because of the high intrinsic fluorescence of EGFP and the association of the fusion protein with the plasma membrane (data not shown). The steady-state distribution of the B-50/EGFP protein was identical to the distribution of B-50 in wt PC12 cells or of transfected B-50 in PC-B2 cells after immunofluorescent labeling. This indicated that the B-50/EGFP construct behaved similarly to the wt protein. Cells expressing B-50/EGFP displayed numerous filopodia extruding from a stable, substrate-attached base (Fig. 3A). Whereas some of the filopodial extensions appeared to be immobile and remained attached to the substrate (Fig. 3A, arrows), others were swaying around in the culture medium confirming their filopodial nature (Fig. 3A, filopodia near arrowheads). Time-lapse experiments of blebbing cells, induced by expression of high levels of B-50/EGFP, revealed the dynamic state of the cellular surface. Bleb formation was rapid,

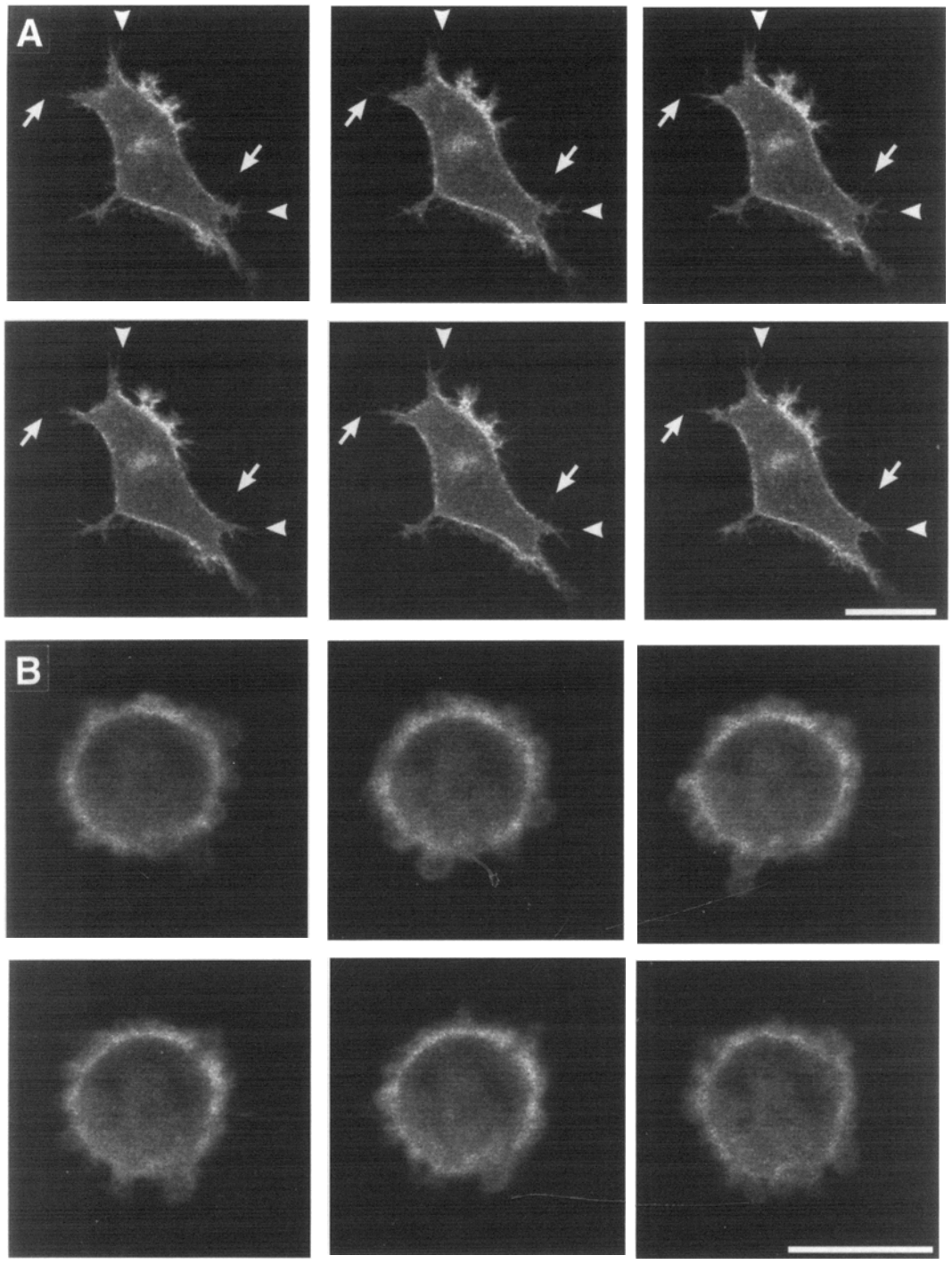

Fig. 3. Motility of B-50-induced cell-surface extensions in PC-B2 cells. PC-B2 cells were grown on 24-mm collagen-coated glass cover slips, transfected with a B-50/EGFP fusion construct, differentiated with NGF for 48 h and observed by time-lapse confocal microscopy. Frames show B-50/EGFP fluorescence in a representative **(A)** filopodial or **(B)** blebbing cell at 20-s time intervals from upper left to lower right frame. Arrows and arrowheads in **(A)** designate stable or motile filopodia respectively. Scale bar, 10 μm.

smooth, and regular; maximal size was usually reached within 20–40 s. After cessation of expansion of primary blebs, subsequent blebs often appeared immediately, either from the apical surface of the first bleb (*see* frame 3; Fig. 3B) or next to its base (*see* frame 6; Fig. 3B). After reaching the maximal volume, each bleb remained extended for 10–20 s and then slowly retracted over the next 40–60 s to become stabilized at a much smaller size.

Discussion

Several studies have reported that B-50 transfection causes formation of filopodia and blebs in a variety of cell types *(3,4,6,7,17,25,31)*. In this study, we have elaborated on these findings and show that the B-50-induced increase in cell-surface activity is correlated with local intracellular accumulations in B-50.

Transfection of neuronaly differentiated PC-B2 cells with B-50 evoked a profound modulation of the cortical actin cytoskeleton and caused extrusion of dynamic filopodia or blebs at sites with elevated levels of B-50. Local high concentrations of B-50 at the plasma membrane are associated with a local increase in f-actin (as shown by phalloidin), which was accompanied by the extrusion of numerous filopodia from growth cone-like structures (Fig. 1A, B). This is particularly interesting, since steering events in moving growth cones are preceded by local accumulations of actin filaments within stabilized filopodia at sites of future growth (for review, *see 32)* and suggests that local accumulation of B-50 could initiate growth cone steering. This is corroborated by the lack of local f-actin concentrations in growth cones and outgrowth/steering problems of antisense B-50 oligonucleotide-treated dorsal root ganglion neurons *(12)*.

When local levels of B-50 further increased, a distinct morphological effect in PC-B2 cells was observed, i.e., formation of numerous, highly motile blebs (Figs. 1C,D, 2B,C). Blebs are common features at the periphery of eukaryotic cells during mitosis, spreading, and at the leading edge of migrating cells. Blebs alternate with other protrusions, such as ruffles, suggesting that a similar protrusive force is involved *(33)*. The presence of both f-actin-positive and negative blebs in B-50-transfected cells (Fig. 2B) may reflect differences in the maturation state. Newly formed blebs are devoid of f-actin, whereas mature and stabilized blebs exhibit high levels of actin filaments *(33)*. Bleb formation presumably starts when fluid-driven expansion outpaces the local rate of actin polymerization and ceases when cortical actin gelation is achieved *(33)*. B-50-induced bleb formation may be caused either by a local reorganization of the cortical actin cytoskeleton leading to a partial dissociation of the local actin network and/or to a disconnection from the plasma membrane to which B-50 is attached. The virtual absence of colocalization of B-50 and actin filaments at bleb membranes (Fig. 1C, 1D; right panels) implies a local disconnection of the plasma membrane from the underlying actin cytoskeleton, setting the pace for bleb formation.

Ultrastructural localization of B-50 confirmed that the protein was concentrated mainly at the plasma membrane of morphologically active regions, i.e., of filopodia and blebs. The poor preservation of the actin cytoskeleton in sections processed for immunogold labeling *(34)* precluded ultrastructural colocalization of B-50 and actin filaments within transfected cells. Frequently, the bleb interior contained less dense material than the cytosol, arguing for the existence of a selective barrier. This barrier may be formed either by a membrane and/or by bundles of actin filaments *(6)*. Within blebs, we frequently observed electron-lucent, B-50-decorated vesicular structures that may represent either transport vesicles, endocytic/pinocytic structures, or invaginated membrane extensions. It is, however, unclear what the precise nature of these vesicular profiles inside the blebs is. Transfection of B-50 in the PC-B2 cells leads to the initiation of bleb formation. Thus, some of the vesicular profiles will certainly be transport vesicles. The size of most of the vesicular profiles in the electron-light blebs is, how-

ever, too big to represent transport vesicles. If there is also a real physical barrier in the blebs with a more electron-light appearance, then the nature of the profiles must either be endocytic/pinocytic or invaginated membranes. We have recently shown that transfection of B-50 in rat fibroblasts leads to an enhanced pinocytic activity *(35)*. B-50 colocalized in these pinosomes with Thy-1, a GPI-anchored protein associated with specialized lipid microdomains termed rafts *(36,37)*. B-50 has also been shown to be present in rafts by the Triton X-100 insolubility criterion *(38,39)*, and we recently showed that B-50 is also present in raft membranes in vivo *(35)*. Like our present data, motile fibroblasts transfected with B-50 also exhibited high concentrations of B-50 at the leading edge of ruffling membranes, which coincided with actin polymerization. The exact relation among the raft membrane, B-50, and the actin cytoskeleton is, however, unknown.

From the present data, we conclude that local increases in B-50 concentration evoke a reorganization of the cortical actin cytoskeleton that is accompanied by locally increased cell-surface activity, resulting in formation of filopodia and blebs. The mechanisms underlying B-50-induced modulation of the actin cytoskeleton are still largely unknown. In vitro, B-50 cosedimented with actin filaments *(26–28)* and influenced actin polymerization depending on the phosphorylation state of the protein *(26)*. The high degree of colocalization of B-50 and f-actin in various cell types suggests that such an interaction may also occur *in situ (3,12,17,25)*. However, no apparent differences were observed between morphology or f-actin distribution in PC-B2 cells transfected with PKC-phosphorylation site mutants (S41A, S41D) compared to cells transfected with wt B-50 (data not shown). This implies that the state of the PKC phosphorylation site does not considerably alter subcortical actin dynamics in NGF-differentiated PC12 cells *in situ*. Recently, we have demonstrated that B-50-induced filopodia formation in spreading fibroblasts depend on Rho-GTPase function. Members of the Rho family of GTPases are assumed to be key regulators of the activity of the actin cytoskeleton in all eukaryotic cells *(40,41)*. Interestingly, apoptotic membrane blebbing was shown to be inhibited by exogenous addition of C3-transferase, a specific inhibitor of Rho function *(42)*. Whether the B-50-induced reorganization of the cortical actin cytoskeleton and formation of filopodia and blebs in PC12 cells depend on the Rho-GTPase remains to be established.

Acknowledgments

We are grateful to W. J. Hage of the Netherlands Institute for Developmental Biology for excellent technical support with the confocal laser scanning microscope. This work was supported by the Netherlands Organization for Scientific Research (MW-NWO grant 903-42-006) and by the "Prinses Beatrix Fonds" (grant 95–1008).

References

1. Skene J. H. and Willard M. B. (1981) Characteristics of growth-associated polypeptides in regenerating toad retinal ganglion cell axons. *J. Neurosci.* **1,** 419–426.
2. Skene J. H. P. (1989) Axonal growth-associated proteins. *Ann. Rev. Neurosci.* **12,** 127–156.
3. Aarts L. H. J., Schrama L. H., Hage W. J., Bos J. L., Gispen W. H., and Schotman P. (1998) B-50/GAP-43-induced formation of filopodia depends on Rho-GTPase *Mol. Biol. Cell* **9,** 1279–1292.
4. Strittmatter S. M., Valenzuela D., and Fishman M. C. (1994) An amino-terminal domain of the growth-associated protein GAP-43 mediates its effects on filopodial formation and cell spreading. *J. Cell Sci.* **107,** 195–204.
5. Verhaagen J., Hermens W. T. J. M. C., Oestreicher A. B., Gispen W. H., Rabkin S. D., Pfaff D. W., et al. (1994) Expression of the growth-associated protein B-50/GAP43 via a defective herpes-simplex virus vector results in profound morphological changes in non-neuronal cells. *Mol. Brain Res.* **26,** 26–36.
6. Wiederkehr A., Staple J., and Caroni P. (1997) The motility-associated proteins GAP-43, MAR-

CKS, and CAP-23 share unique targeting and surface activity-inducing properties. *Exp. Cell Res.* **236,** 103–116.
7. Zuber M. X., Goodman D. W., Karns L. R., and Fishman M. C. (1989) The neuronal growth-associated protein GAP-43 induces filopodia in non-neuronal cells. *Science* **244,** 1193–1195.
8. Morton A. J. and Buss T. N. (1992) Accelerated differentiation in response to retinoic acid after retrovirally mediated gene transfer of GAP-43 into mouse neuroblastoma cells. *Eur. J. Neurosci.* **4,** 910–916.
9. Yankner B. A., Benowitz L. I., Villa-Komaroff L., and Neve R. L. (1990) Transfection of PC12 cells with the human GAP-43 gene: effects on neurite outgrowth and regeneration. *Mol. Brain Res.* **7,** 39–44.
10. Kumagai C., Tohda M., Isobe M., and Nomura Y. (1992) Involvement of growth-associated protein-43 with irreversible neurite outgrowth by dibutyryl cyclic AMP and phorbol ester in NG 108–15 cells. *J. Neurochem.* **59,** 41–47.
11. Aigner L. and Caroni P. (1993) Depletion of 43-kD growth-associated protein in primary sensory neurons leads to diminished formation and spreading of growth cones. *J. Cell Biol.* **123,** 417–429.
12. Aigner L. and Caroni P. (1995) Absence of persistent spreading, branching, and adhesion in GAP-43-depleted growth cones. *J. Cell Biol.* **128,** 647–660.
13. Jap Tjoen San E. R. A., Schmidt-Michels M. H., Oestreicher A. B., Gispen W. H., and Schotman P. (1992) Inhibition of nerve growth factor-induced B-50/GAP-43 expression by antisense oligomers interferes with neurite outgrowth of PC12 cells. *Biochem. Biophys. Res. Commun.* **187,** 839–846.
14. Shea T. B., Perrone-Bizzozero N. I., Beermann M. L., and Benowitz L. I. (1991) Phospholipid-mediated delivery of anti-GAP-43 antibodies into neuroblastoma cells prevents neuritogenesis. *J. Neurosci.* **11,** 1685–1690.
15. Greene L. A., Sobeih M. M., and Teng K. K. (1991) Methodologies for the culture and experimental use of the PC12 rat pheochromocytoma cell line, in *Culturing Nerve Cells* (Banker G. and Goslin K., eds.) Massachuchetts Institute of Technology, Cambridge, MA, pp. 207–226.
16. Van Hooff C. O. M., Holthuis J. C. M., Oestreicher A. B., Boonstra J., De Graan P. N. E., and Gispen W. H. (1989) Nerve growth factor-induced changes in the intracellular localization of the protein kinase C substrate B-50 in pheochromocytoma PC12 cells. *J. Cell Biol.* **108,** 1115–1125.
17. Nielander H. B., French P., Oestreicher A. B., Gispen W. H., and Schotman P. (1993) Spontaneous morphological changes by overexpression of the growth-associated protein B-50/GAP-43 in a PC12 cell line. *Neurosci. Lett.* **162,** 46–50.
18. Jap Tjoen San E. R. A., Van Rozen A. J., Nielander H. B., Oestreicher A. B., Gispen W. H., and Schotman P. (1995) Expression levels of B-50/GAP-43 in PC12 cells are decisive for the complexity of their neurites and growth cones. *J. Mol. Neurosci.* **6,** 185–200.
19. Baetge E. E. and Hammang J. P. (1991) Neurite outgrowth in PC12 cells deficient in GAP-43. *Neuron* **6,** 21–30.
20. Skene J. H. P. and Virág I. (1989) Posttranslational membrane attachment and dynamic fatty acid acylation of a neuronal growth cone protein, GAP-43. *J. Cell Biol.* **108,** 613–624.
21. Aarts L. H. J., Van der Linden J. A. M., Hage W. J., Van Rozen A. J., Oestreicher A. B., Gispen W. H., et al. (1995) N-terminal cysteines essential for Golgi sorting of B-50 (GAP-43) in PC12 cells. *Neuroreport* **6,** 969–972.
22. Liu Y., Chapman E. R., and Storm D. R. (1991) Targeting of neuromodulin (GAP-43) fusion proteins to growth cones in cultured rat embryonic neurons. *Neuron* **6,** 411–420.
23. Liu Y., Fisher D. A., and Storm D. R. (1994) Intracellular sorting of neuromodulin (GAP-43) mutants modified in the membrane targeting domain. *J. Neurosci.* **14,** 5807–5817.
24. Zuber M. X., Strittmatter S. M., and Fishman M. C. (1989) A membrane-targeting signal in the amino terminus of the neuronal protein GAP-43. *Nature* **341,** 345–348.
25. Widmer F. and Caroni P. (1993) Phosphorylation-site mutagenesis of the growth-associated protein GAP-43 modulates its effects on cell spreading and morphology. *J. Cell Biol.* **120,** 503–512.
26. He Q., Dent E. W., and Meiri K. F. (1997) Modulation of actin filament behavior by GAp-43 (neuromodulin) is dependent on the phosphorylation status of serine 41, the protein kinase C site. *J. Neurosci.* **17,** 3515–3524.
27. Hens J. J. H., Benfenati F., Nielander H. B., Valtorta F., Gispen W. H., and De Graan P. N. E. (1993) B-50/GAP-43 binds to actin filaments without affecting actin polymerization and filament organization. *J. Neurochem.* **61,** 1530–1533.

28. Strittmatter S. M., Vartanian T., and Fishman M. C. (1992) GAP-43 as a plasticity protein in neuronal form and repair. *J. Neurobiol.* **23,** 507–520.
29. Mercken M., Lubke U., Vandermeeren M., Gheuens J., and Oestreicher A. B. (1992) Immunocytochemical detection of the growth associated protein B-50 by newly characterized monoclonal antibodies in human brain and muscle. *J. Neurobiol.* **23,** 309–321.
30. Danscher G. (1981) Localization of gold in biological tissue. A photochemical method for light and electronmicroscopy. *Histochemistry* **71,** 81–88.
31. Meiri K. F., Hammang J. P., Dent E. W., and Baetge E. E. (1996) Mutagenesis of ser41 to ala inhibits the association of GAP-43 with the membrane skeleton of GAP-43-deficient PC12B cells: effects on cell adhesion and the composition of neurite cytoskeleton and membrane. *J. Neurobiol.* **29,** 213–232.
32. Tanaka E. and Sabry J. (1995) Making the connection: Cytoskeletal rearrangements during growth cone guidance. *Cell* **83,** 171–176.
33. Cunningham C. C. (1995) Actin polymerization and intracellular solvent flow in cell surface blebbing. *J. Cell Biol.* **129,** 1589–1599.
34. Bridgman P. C., Lewis A. K., and Victor J. C. (1993) Comparison of the ability of freeze etch and freeze substitution to preserve actin filament structure. *Microsc. Res. Tech.* **24,** 385–394
35. Aarts L. H. J., Verkade P., Van Dalen J. J. W., Van Rozen A. J., Gispen W. H., Schrama L. H., et al. (1999) B-50/GAP-43 potentiates cytoskeletal reorganization in raft domains. *Mol. Cell. Neurosci.* **14,** 85–97.
36. Simons K. and E. Ikonen (1997) Sphingolipid-cholesterol rafts in membrane trafficking and signalling in raft domains. *Nature* **387,** 569–572.
37. Brown D. A. and E. London (1998) Functions of lipid rafts in biological membranes. *Annu. Rev. Cell Dev. Biol.* **14,** 111–136.
38. Maekawa S., Kumanogoh H., Funatsu N., Takei N., Inoue K., Endo Y., et al. (1997) Identification of NAP-22 and GAP-43 (neuromodulin) as major protein components in a Triton insoluble low density fraction of rat brain. *Biochim. Biophys. Acta* **1323,** 1–5.
39. Arni S., Keilbaugh S. A., Ostermeyer A. G., and Brown D. A. (1998). Association of GAP-43 with detergent-resistant membranes requires two palmitoylated cysteine residues. *J. Biol. Chem.* **273,** 28478–28485.
40. Mackay D. J. G., Nobes C. D. and Hall A. (1995) The Rho's progress: A potential role during neuritogenesis for the Rho family of GTPases. *Trends Neurosci.* **18,** 496–501.
41. Symons M. (1996) Rho family GTPases: The cytoskeleton and beyond. *Trends Biochem. Sci.* **21,** 178–181.
42. Mills J. C., Stone N. L., Erhardt J. and Pittman R. N. (1998) Apoptotic membrane blebbing is regulated by myosin light chain phosphorylation. *J. Cell Biol.* **140,** 627–636.